

## Thermophilic Anaerobic Digestion of Pig Dung with Snail Shell Additive Supplementation for Enhanced Biogas Production

Ndibe Izuchukwu Onyekachukwu<sup>1\*</sup>, Ifeoma Amaoge Obiora-Okafo<sup>1</sup>, Matthew Ndubuisi Abonyi<sup>1</sup>

<sup>1</sup>Department of Chemical Engineering, Nnamdi Azikiwe University, Awka, Nigeria

\*Corresponding Author's E-mail: [io.ndibe@unizik.edu.ng](mailto:io.ndibe@unizik.edu.ng)

---

### Abstract

The study investigated the thermophilic anaerobic digestion of pig dung with snail shell as additive for enhanced biogas production. Pig dung and additive was weighed and mixed with distilled water in a 500 ml round-bottom flask. The flask containing the slurry was connected to a Soxhlet extractor workstation, and was placed in a heating mantle. When heat was applied, the gas was conveyed through the thimble to the shell and tube heat exchanger, where the gas was condensed. The results show that the optimal conditions for biogas production were additive dosage at 3.5 g, pig dung/ water ratio at 0.16 g/ml, time at 60 mins and temperature at 70°C, under these conditions the biogas yield was 24.45 %. CCD of RSM was applied to enhance process optimization and predict the optimal outcome. The model demonstrated significant results, with a p-value of less than 0.0001. The R<sup>2</sup> of 0.9835, ANOVA results indicate that the model effectively describes the anaerobic digestion of pig dung for biogas production. The produced biogas contains 66.9% methane and 27.2% CO<sub>2</sub> by volume with other constituents present as shown by gas chromatography and FTIR, therefore, the feedstocks used in this study have the potential to support the efficient and sustainable operation and production of biogas plants on a large scale.

**Keywords:** Thermophilic, Biogas, Pig dung, Snail shell, Optimization

---

### 1. Introduction

The world's constant environmental changes are caused by the burning of fossil fuels (coal, oil, gas) and overexploitation of natural resources. Global urbanization, economic and industrial developments are creating solid waste that the Earth cannot cope with (Ignatowicz et al., 2023). The continuous increase in the production of solid waste, including sewage sludge, is a problem, and solving it has become an environmental priority. In response to the problem of growing organic waste deposits and the need for new renewable energy sources, a number of scientific initiatives have been developed to explore the energy potential of bio-waste for biogas production. The reuse of bio-solids, such as sewage sludge, agricultural and industrial waste, is highly beneficial and reduces landfill and soil pollution (Ignatowicz et al., 2023).

Energy plays a pivotal role in driving economic growth in the 21st century, and a lack of sufficient energy resources can hinder the socio-economic progress of a nation. In Nigeria, the demand for energy is steadily increasing. Historically, fossil fuels have powered the industrial revolution, leading to significant advancements in technology, economy, and society. However, their use has also had detrimental environmental consequences, such as contributing to climate change (Okonkwo et al., 2021). As a result, there is now a global shift toward reducing reliance on fossil fuels and promoting the development and use of renewable energy sources as a key element of sustainable energy strategies (Okonkwo et al., 2021). According to the International Energy Agency (IEA), renewable energy refers to energy derived from natural processes that are replenished more quickly than they are consumed (Okonkwo et al., 2021). Renewable technologies produce power, heat or mechanical energy using

biomass (energy crops, agricultural or forestry residues, biogenic municipal waste, etc.), wind, solar (thermal and photovoltaic), hydro (river flow, tides, waves), and geothermal energy (Okonkwo et al., 2021; Kasinath et al., 2021). Renewable energy is an environmentally friendly energy source that generates minimal or no pollution (Chilakpu, 2015).

Biogas is a clean renewable energy produced from organic wastes using anaerobic digestion as a method. Biogas is generated when organic matter (bio-waste) decomposes in an oxygen-free environment through microbial activity, a process known as anaerobic digestion (Khalil et al., 2019). Converting waste into energy, particularly by producing biogas from animal waste, is recognized as an effective approach to achieving sustainable energy development goals in numerous developing nations (Khalil et al., 2019). The biogas potential of organic waste in Nigeria has been evaluated and shows significant promise for contributing to energy production and biofertilizer generation for household use (Ngumah et al., 2013).

Anaerobic digestion is a multi-stage biological process that breaks down and stabilizes organic matter in the absence of oxygen. Through the activity of diverse groups of anaerobic microorganisms, various organic materials can be transformed into biogas, a renewable energy source primarily composed of methane ( $\text{CH}_4$ ) and carbon dioxide ( $\text{CO}_2$ ). This biogas can serve as an alternative to fossil fuels for generating heat or electricity. Additionally, biogas plants can process organic waste, reducing environmental pollution while recovering energy (Wu et al., 2019). Pig dung, a byproduct of pig farming, is a significant waste material. In Nigeria, approximately 5.2 million kilograms of pig manure are produced daily. If not managed properly, this waste poses serious environmental and health risks (Itodo et al., 2001). The primary pollutants in pig production are nitrogen and phosphorus, which are also key substrates for biogas production. Phosphorus contributes to the eutrophication of water bodies, while nitrogen leads to methane emissions and acid rain, exacerbating environmental challenges (Ofomatah et al., 2021).

The use of additives has been shown to offer marked improvements in anaerobic digestion performance as it not only increases biogas production but also reduces air pollution during the production (Liu et al., 2021). Snail shell has been identified as an agricultural by-product and as one of the world's most serious agricultural waste and pollutants, particularly in countries where snails are more prevalent. According to Kuttner et al., (2015) the addition of Calcium carbonate which is a major component of snail shell increased performance and biogas production by 8%. The shell has about 95% by weight of  $\text{CaCO}_3$  crystalline and 5% organic matter (Zuliantoni et al 2022).

The use of thermophilic temperature in this experiment makes it significant because it leads to increased reaction rate, helps break down organic matter in pig dung and significantly accelerate the biochemical reaction leading to faster biogas production. Thermophilic anaerobic digestion offers the potential for increased biomethane production, as well as a more stable organic output and pathogen-free effluent compared to traditional mesophilic digestion (Labatut et al., 2014). This research focuses on enhancing biogas production from bio-waste through anaerobic digestion by employing Central Composite Design (CCD) of Response Surface Methodology (RSM), a predictive modeling tool. The study investigates the use of pig dung and ground snail shell as an additive under thermophilic conditions, utilizing Central Composite Design in the anaerobic process. The outcomes of this study could assist biogas facility operators in refining their decision-making processes, particularly if the predictive model is incorporated into their operations. This innovative approach on the use of animal, agricultural waste (pig dung and snail shell) as the feedstock and additive respectively for biogas production will help reduce environmental pollution associated with indiscriminate disposal of these waste and energy production.

## **2.0 Materials and methods**

### **2.1 Collection and Pretreatment of Feedstock**

The feedstock used in this study was collected from a pig farm in Amansea in Awka south LGA of Anambra state. The Pig dung was scraped from the floor of the Pig farm house with a shovel and then bagged. The sample was sun dried for 36 hrs. 1kg of the Pig dung was taken to chemical Engineering laboratory Nnamdi Azikiwe University, Awka for characterization and for the slurry preparation to be used in the experiment. The snail shell used in this study are the giant west African snail (*Archachatina marginata*) and were collected with clean polythene bags from Eke market, Awka which weighed 4 kg. The snail shells were crushed into smaller pieces with mortar and pestle and then it was soaked in 10 L of clean tap water for 3 days and then washed to remove all the impurities. They were then dried under the sun for 24 hrs to remove the excess water. The snail shells were ground mechanically using 2

hp electric grinding mill machine to obtain the fine powder. The powder obtained was passed through 500  $\mu\text{m}$  sieve mesh to obtain particles size less than 500  $\mu\text{m}$ . The powdered snail shell weighed 500 g.

## 2.2 Characterization of The Pig Dung

### 2.2.1 Total Solids Determination

The determination of total solids (TS) followed the method outlined by Wellington et al., (2017). A 10 g portion of each fresh sample was placed in a porcelain cup and measured using a weighing scale. The samples were then dried in an incubator at  $105 \pm 5$  °C for six hours before being reweighed. The total solids (dry matter) content was calculated using the following equation:

$$TS\% = \frac{W_d}{W} \times 100 \quad (1)$$

Where  $w_d$  represents the weight of Dried sample (g) and W is the initial sample weight (g)

### 2.2.2 Determination of The Ash Content

The mineral content of the raw waste is often determined through this method. Following the AOAC (1990) procedure, 5 grams of finely ground samples were weighed and placed into pre-washed porcelain crucibles. These crucibles were dried in an oven at 100°C, cooled in a desiccator, and weighed. The samples were then heated in a muffle furnace at 600°C for 4 hours. After heating, they were removed, cooled in a desiccator, and weighed again.

$$\%Ash = \frac{A - B}{C} \times \frac{100}{1} \quad (2)$$

A = Weight of crucible + ash

B = Weight of crucible

C = Weight of original sample

### 2.2.3 Moisture Content Determination

The moisture content of the feedstock was calculated following the APHA, (2005) method. Moisture content refers to the mass of water present in the material, typically expressed as a percentage of the total weight. The crucible was thoroughly cleaned, dried in an oven at 105°C for approximately 30 minutes, and then allowed to cool to room temperature. The weight of the empty, dried crucible was recorded ( $W_1$ ). A wet sample of each substrate was placed in the crucible and dried in the oven at 105°C for about 3 hours until a constant weight was achieved ( $W_2$ ). After cooling to room temperature, the crucible and the dried feedstock were weighed again ( $W_3$ ). The moisture content was determined using the following formula:

$$MC = \frac{(W_2 - W_1) - (W_3 - W_1)}{(W_2 - W_1)} \times 100\% \quad (3)$$

### 2.2.4 Determination of Volatile Matter

A muffle furnace was utilized to measure the volatile matter content of the sample. A 5 g sample was weighed beforehand. Volatile matter refers to the portion of the material that, when heated in the absence of air under specific conditions, is released as gases and vapors. Each pre-weighed sample underwent dry oxidation in the muffle furnace at 550°C for 10 minutes. After heating, the sample was removed and cooled in a desiccator. This process was repeated in triplicate, with each sample cooled in the desiccator. The final weight of the sample was recorded using an electronic weighing balance. The volatile matter content was calculated using the following formula:

$$\%VM = \left( \frac{w_i - w_f}{w_i} \right) \times 100 \quad (4)$$

where,  $w_i$  = initial weight of the sample (before dry oxidation),  $w_f$  = final weight of the sample (after dry oxidation).

### 2.2.5 Determination of the Fixed Carbon Content of the Sample

The fixed carbon of the sample was determined by using Equation:

$$\%FC = 100\% - \%Ash - \%VM \quad (5)$$

where,

%Ash = Determined ash contents, %VM = Determined volatile matters

### 2.2.6 Determination of Energy Value

The energy value of the sample was determined using a laboratory canister, following the procedure described by Onuora et al., (2023). An Oxygen Bomb Calorimeter (model XRY-1A) was used for the analysis. The sample, along with a 10 cm ignition wire, was weighed. Both ends of the ignition wire were attached to two electrode poles, ensuring proper contact with the sample. The oxygen bomb was filled with 10 mL of distilled water, securely sealed, and pressurized with oxygen at 2.8–3.0 MPa. The oxygen bomb was then placed inside the clamp within the inner canister, and all necessary wiring connections were made. A temperature sensor was inserted into the canister. After switching on the power and stir functions, the water was stirred for two minutes, and the initial temperature ( $T_0$ ) was recorded. The fire button was then activated, allowing the instrument to automatically measure and store data until the test duration reached 31 seconds. The final temperature ( $T_f$ ) was then recorded. Following the test, stirring was stopped, the temperature sensor was removed, and the oxygen bomb was opened after releasing the internal oxygen pressure. The remaining length of the unburned ignition wire was measured. The bomb's inner lining was rinsed with distilled water, and a few drops of methyl red indicator were added. The solution was then titrated with 0.0709 N sodium carbonate, and the volume of alkali consumed was recorded.

The heat of combustion was calculated,

$$\text{Calorific value} = \frac{E\Delta T - \Phi - V}{M} \quad (6)$$

Where E = Energy equivalent of the calorimeter,  $\Phi$  = Correction for heat of combustion of the firing wire,  $\Delta T$  = Change in temperature, V = Volume of standard alkali solution (in milliliters), M = Mass of the sample being evaluated.

### 2.3 Instrumental Characterization on Snail Shell:

The functional groups in the snail shell were identified using Fourier Transform Infra-red (FTIR) analysis and done with FTIR – 990 FTIR Spectrometer. The chemical (Elemental/oxide) composition was examined by Energy Dispersive X-ray fluorescent (XRF) using MESA – 50K X-RAY fluorescence analyzer. The phase constituent was analyzed using X-ray diffractometer (XRD) and examined with LR-8270 mini benchtop X-ray diffractometer.

### 2.4 Biogas Experimental Procedure and Laboratory Set Up of The Digester

Thermophilic anaerobic digestion method was employed in this experiment for the production of the biogas. Fine powdered pig dung was weighed and mixed with distilled water in a 500 ml round-bottom flask. The snail shell was added as additive. The slurry mixture was thoroughly mixed using a stirring rod to ensure uniformity. The flask containing the slurry was connected to a soxhlet extractor workstation, which comprises of the soxhlet extraction thimble and reflux condenser with water inlet and outlet source, while the flask was placed in a heating mantle. When heat was applied, the gas was conveyed through the thimble to the shell and tube heat exchanger, where the gas was condensed. The condensed gas was collected at thimble for further processing (dehydration) and analysis. Method of gas dehydration using solid desiccant was employed in determining the biogas yield.

The influence of process parameters, including the pig dung-to-water ratio, catalyst dosage, temperature, and time, on biogas production was assessed using an experimental design matrix. Response surface methodology (RSM) was then used to optimize the biogas yield.

Silica gel ( $\text{SiO}_2$ ) Blue coarse was used as the dehydrating agent (desiccant) in a U- tube. It absorbs the water while the gas was released (Generowicz, 2020).

To calculate the percentage biogas yield:

$$\% \text{ Biogas yield} = \frac{Q}{C} \times 100 \quad (7)$$

The quantity of gas released Q:

$$Q = D - W \quad (8)$$

Condensed gas which is a mixture of water and gas = D

Weight of substrate used = C

Quantity of water in the condensed gas W:

$$W = W_2 - W_1 \quad (9)$$

Where  $W_1$  represents the weight of silica gel before use (g), and  $W_2$  denotes the weight of silica gel after use (g).

## 2.5 Characterization of Biogas Produced

### 2.5.1 Determination of Biogas Quality and Composition

The analysis of Gas Constituents was performed on a BUCK M910 Gas chromatography equipped with a FID detector. A RESTEK 15 meter MXT-1 column (15m x 250um x 0.15um) was used. The injector temperature was 280°C with splitless injection of 2ul of sample and a linear velocity of 30cms<sup>-1</sup>, Helium 5.0 Pa.s was the carrier gas with a flow rate of 40ml/min. The oven operated initially at 200°C, it was heated to 330°C at a rate of 3°C min<sup>-1</sup> and was kept at this temperature for 5min, the detector operated at a temperature of 320°C. 0.5ul of the extracted sample was injected into the equipment via the injector of the equipment and allowed to scan Gas components for 45 minutes. The composition of gases was analyzed by calculating the ratio between the area and mass of the internal standard and the area of the identified compounds. The concentration of the various gas components was expressed in µg/mL.

### 2.5.2 Fourier Transform Infrared (FTIR) Spectroscopic Characterization

The functional groups present in the produced biogas were identified using Fourier Transform Infrared (FTIR) spectroscopy. An FTIR spectrophotometer was utilized to analyze the functional groups. The FTIR spectrum was recorded in transmission mode, employing the KBr pellet technique. During the process, the Fourier transform algorithm converted the raw data into a detailed spectrum featuring distinct peaks. These peaks were analyzed to determine the specific functional groups associated with the biogas.

## 3.0 Result and Discussion

### 3.1 Proximate Analysis of Pig Dung

The proximate analysis results of the pig dung sample are shown in Table 1. The moisture content was within the recommended limit of 10% or less for long-term storage (Onuora et al., 2023). A lower moisture content improves storage stability by inhibiting mold growth and minimizing biochemical reactions that depend on moisture. Ash content of 5.83%, was recorded, which is an indication of the high mineral content of the samples showing more organic material is available to produce biogas (Onuora et al., 2023). Low moisture and ash content will result in high organic matter content and therefore high biogas yield. Volatile matter content value of 74.56% which signifies their suitability for biogas production as recorded by other authors. The energy value range is suitable for energy generation through anaerobic digestion. The total solids content of 90.53% is important because it shows pig dung contains more biodegradable material, which will eventually lead to a higher biogas yield (Godfrey, 2024).

**Table 1: Proximate analysis result**

Parameters	Pig dung (PD)
Volatile matter content (%)	74.56
Ash content (%)	5.83
Moisture content (%)	9.47
Fixed carbon (%)	10.14
Energy Value (kJ/100g)	2588.15
Total Solids (%)	90.53

### 3.2 Instrumental Characterization of Snail Shell

#### 3.2.1 XRD Result of Snail Shell

The results of the phase composition investigated by X-ray diffractometer is presented in Fig. 1a and Fig. 1b. The XRD pattern obtained revealed that the diffraction peaks is 36.3569° and the inter-planar distance is 2.47113Å with a relative intensity of the X-ray scattering of 100.00. The phases at these peaks is aragonite with a score of 27, respectively. The presence of these minerals in the shell forms the bases of the hard nature of the shells. Mineralogical constitution of the snail shells, as determined by X-ray diffraction (XRD) XRD reveals a high proportion of calcium carbonate (CaCO<sub>3</sub>), predominantly aragonite (75.56%), trace amounts of lime (CaO), quartz (SiO<sub>2</sub>), periclase (MgO), and orthoclase (KAlSi<sub>3</sub>O<sub>8</sub>). Presence of calcium carbonate (CaCO<sub>3</sub>) and lime (CaO) in snail shells supports neutralization of acidic surroundings, preventing process instability due to volatile fatty acid (VFA) accumulation (Liu et al., 2022). Snail shell Calcium (Ca<sup>2+</sup>) and Magnesium (Mg<sup>2+</sup>) are vital cofactors of microbial enzymes during hydrolysis, acidogenesis, and methanogenesis (Wang et al., 2019). Calcium-based products like snail shells precipitate the ammonium ions (NH<sub>4</sub><sup>+</sup>) in the form of ammonium salts, reducing free ammonia (NH<sub>3</sub>) toxicity and promoting a more healthy microbial population. Alkaline nature of snail shells prevents acidification and creates a stable microbial community, thus contributing to greater production of methane (Ning et al., 2019).

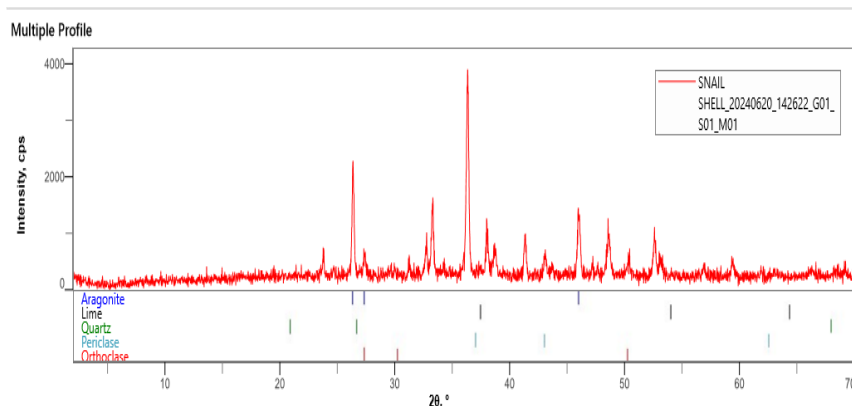


Fig. 1a: XRD pattern of snail shell

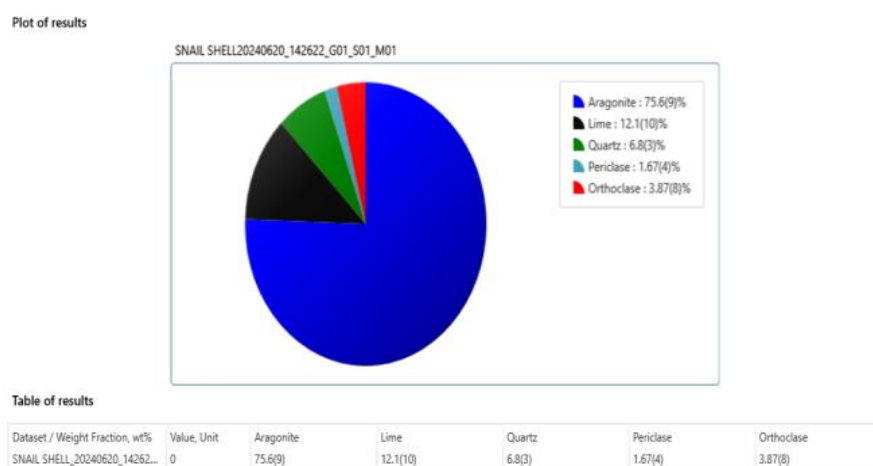
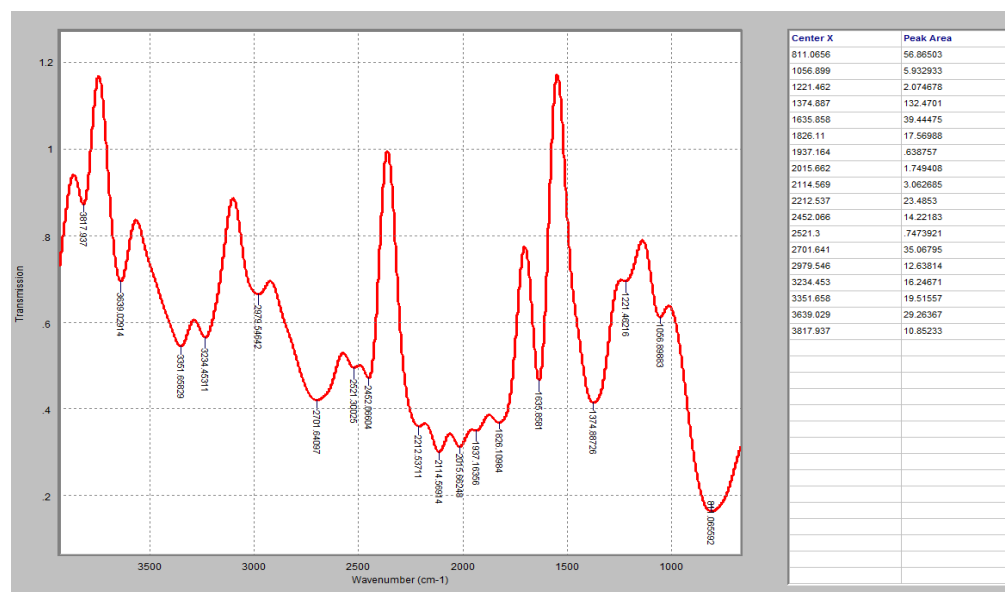


Fig. 1b: XRD plot of snail shell

### 3.2.2 Fourier Transform Infrared (FTIR) Analysis of Snail Shell

The infrared spectra of snail shell, as depicted in Fig. 2, reveal distinct absorption peaks corresponding to  $\text{CO}_3^{2-}$  ions at wavenumbers 1826, 1635, 1374, 1221, 1056, and 811  $\text{cm}^{-1}$ , which are characteristic features of  $\text{CO}_3^{2-}$  in  $\text{CaCO}_3$  (Udomkan and Limswan, 2008). Absorption bands within the range of 1390–1416  $\text{cm}^{-1}$  are attributed to the  $\nu_3(\text{E})$  mode of  $\text{CO}_3^{2-}$  ions, while the absence of the infrared-inactive  $\nu_1(\text{A}_1)$  mode is noted (Zuliantoni et al., 2022). Bands observed between 3234–3817  $\text{cm}^{-1}$  indicate the presence of water content (Sundalian et al., 2021). The peak at 1374  $\text{cm}^{-1}$  corresponds to the  $\nu_1(\text{A}_1)$  vibrational mode of  $\text{CO}_3^{2-}$  ions in the aragonite group. Additionally, the absorption band in the range of 3400–3600  $\text{cm}^{-1}$  results from the stretching vibrations of structural water molecules. This band diminishes with increasing temperature and completely disappears at 400 °C (Udomkan and Limswan, 2008). The vibrations associated with  $\text{CO}_3^{2-}$  ion absorption band are located within the 400 -1800  $\text{cm}^{-1}$  regions. The strong vibration peak at 1423.47 to 1404.09  $\text{cm}^{-1}$  is due to the assigned stretching of vibration of C=O in the carboxylate of  $\text{CaCO}_3$ . The absorption bands observed at the vibration peaks at 811 and 1374  $\text{cm}^{-1}$  are characteristics of calcite (Gbenebor et al., 2017). FTIR analysis confirms that raw snail shell primarily consists of calcium carbonate (aragonite polymorph) with traces of organic compounds and water molecules. This composition makes it a suitable additive for biogas production, as it can help regulate pH, promote microbial activity, and mitigate the inhibitory effects of ammonia and heavy metals (Liu et al., 2022).



**Fig. 2: FTIR spectrum of snail shell**

### 3.2.3 XRF Compositional Analysis

Table 2 shows the result of the oxide composition of the samples using the Energy Dispersive X-Ray Fluorescence (XRF) analysis of snail shell. X-ray Fluorescence (XRF) Spectroscopy is a widely used technique for determining the elemental composition of materials. The provided XRF analysis report for snail shell identifies the presence and concentration of various elements, indicating its mineralogical composition and potential applications in biogas production Owoyemi, & Owoyemi (2020). The result confirmed the presence of  $K_2O$ ,  $Fe_2O_3$ ,  $CaO$ ,  $P_2O_5$ ,  $Al_2O_3$ ,  $ZnO$ ,  $SrO$ ,  $Cr_2O_3$ ,  $TiO_2$ ,  $NiO$ ,  $Ag_2O$ ,  $Pb_2O$ ,  $MnO$  and others as the major constituents of the snail shell sample. This however confirmed the results obtained in Table 2.

It can be observed from Table 2 that the concentration of  $CaCO_3$  of the sample is 89.884% and that of  $Pb_2O$  was the least concentration at 0.002% as gotten by Owoyemi, & Owoyemi (2020). High calcium (Ca) content is expected since snail shells are made up mostly of calcium carbonate ( $CaCO_3$ ) in the aragonite or calcite polymorph. (Kaewdang & Nirunsin, 2019). Magnesium is an important co-factor for enzyme catalyzed reactions of microbial metabolism. Trace elements like silicon, Aluminium, potassium, and iron is required for electron transfer of methanogenic bacteria, improving the anaerobic digestion efficiency (Rao et al., 2022). Silicon (Si) and Aluminum (Al) are commonly found in natural biomineralized materials but are not directly involved in biogas production While Potassium (K) is an essential nutrient for microbial metabolism, particularly for hydrolytic and acidogenic bacteria (Zhou et al., 2020).

**Table 2: XRF Analysis Report**

S/NO	Chemical Formula	Concentration (%)
1	$SiO_2$	0.315
2	$V_2O_5$	0.009
3	$Cr_2O_3$	0.007
4	$MnO$	0.064
5	$Fe_2O_3$	0.154
6	$CoO$	0.044
7	$NiO$	0.023
8	$CuO$	0.075
9	$Nb_2O_5$	0.011
10	$WO_3$	0.043
11	$CaCO_3$	89.884
12	$SO_3$	0.024
13	$MgO$	4.802
14	$K_2O$	0.029

15	Al <sub>2</sub> O <sub>3</sub>	3.122
16	Ta <sub>2</sub> O <sub>5</sub>	0.066
17	Cl	0.392
18	SnO <sub>2</sub>	0.617
19	SrO	0.307
20	Pb <sub>2</sub> O	0.002
21	PbO	0.005

### 3.3 Effects of Various Process Variables on the Biogas Yield

Fig. 4 shows the relationship between temperature (°C) and biogas yield (%), as biogas yield increased as the temperature was increased. The pattern indicates that as the temperature rises from 50°C to around 70°C, biogas production increases, reaching a peak of approximately 25%. Beyond this, any increase in temperature (above 70°C) caused a marginal decline of biogas yield. Furthermore, as process temperatures increase, so does the rate of reactions and the likelihood of inhibition (Labatut et al., 2014). This concurs with findings from previous research on biogas production. For instance, Zhang et al. (2020) explained that mesophilic and thermophilic temperatures exert a marked influence on microbial activity during anaerobic digestion, with optimum biogas production typically observed at approximately 55–70°C before decreasing owing to the heat inhibition of methanogenic bacteria. Similarly, Sambo et al., (1995) explained that the production of biogas was maximum at intermediate thermophilic temperatures (about 70°C) before the production started showing diminishing returns with elevated temperatures. The decrease in biogas production at temperatures above 70°C may result from the denaturation of important microbial enzymes that are essential for anaerobic digestion (Ryue et al., 2020). This observation corroborates the report by Cheng et al., (2018), where it was mentioned that extremely thermophilic conditions (>70°C) disrupt microbial community stability, reducing methanogenic activity.

In Fig. 5, the graph illustrates the trend in time (minutes) and biogas yield (%). The Biogas yield increased as the heating time was raised, after 60 minutes it dropped to a minimal level. There is a linear proportionality between time and biogas yield at the beginning, as the yield increases from approximately 20% at 40 minutes to approximately 25% at 60 minutes. But after the 60-minute peak, the yield will be steady and slightly decline, illustrating a decline of biogas production. This observation aligns with previous research on biogas production dynamics. Zhang et al. (2020) reported that biogas generation initially increases due to microbial activity but eventually stabilizes as substrate availability or environmental conditions become limiting. Ezekoye et al., (2011) indicated that prolonged digestion time beyond the optimum does not necessarily enhance biogas yield and can even cause decreased production rates due to inhibition of microorganisms or substrate restriction. Stabilization recorded at 60 minutes suggests anaerobic digestion process reaches balance, and the production of methane is equal to substrate consumption.

In Fig. 6 the graph shows the relationship between additive dosage (g) and yield of biogas (%). The biogas yields increased as the additive dosage was increasing, it attained the maximum at the catalyst dosage of 3.5 g before it showed a minimal decrease. The pattern is an increase in biogas yield as the dosage of additive increases from 2.5 g to around 3.5 g, where the maximum is attained at around 25%. There is any additional increase in dosage of additive that has no effect on biogas production. This shows that snail shell may have boosted the production of biogas. The catalyst reduces the activation energy, resulting in a higher rate of reaction without being involved in the reaction (Onuora et al., 2023).

The positive correlation in the early phase (2.5 g – 3.5 g) suggests that the additive is positively adding to the anaerobic digestion process. This increase can be attributed to Nutrient Supplementation where Some additives, such as trace metals, enzymes, or buffering agents, trigger microbial activity and improve substrate degradation (Zhang et al., 2020). Snail shell provide methanogenic bacteria with essential nutrients, thereby stimulating biogas production (Liu et al., 2021). Many additives were used in anaerobic digestion and reported dramatically increased biogas and methane production (Çalhan, and Ulutaş, 2023).

It was noticed in Fig. 7 that there was almost linear increase in pig dung/water ratio to the peak of 0.20 and after which a significant decrease was observed. the steady rise in biogas yield from approximately 12% to 25% suggests that increased concentration of pig dung enhances microbial activity and substrate availability. More pig dung content provides more amounts of biodegradable organic matter, leading to greater methane production (sambo et al., 1995).

Above 0.20 g/ml, the increase in the biogas yield does not continue but rather goes down slightly. Too much quantity of pig dung will generate excessive organic load, and thus microbial inhibition occurs due to volatile fatty acids formation. Anaerobic digestion requires sufficient water for microbial metabolism; high solids can restrict microbial mobility and slow degradation (KeChrist et al., 2017).

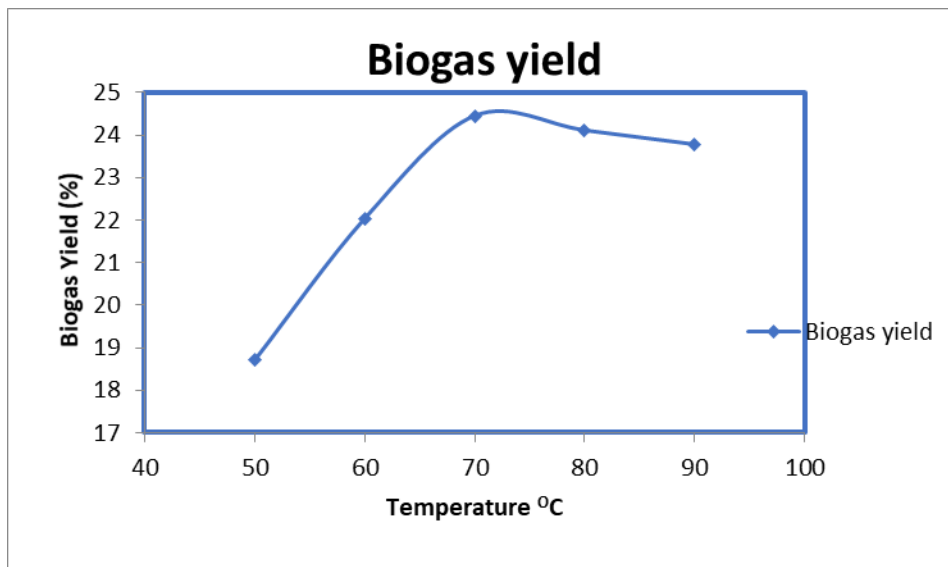


Fig. 4: Effect of temperature on the biogas yield

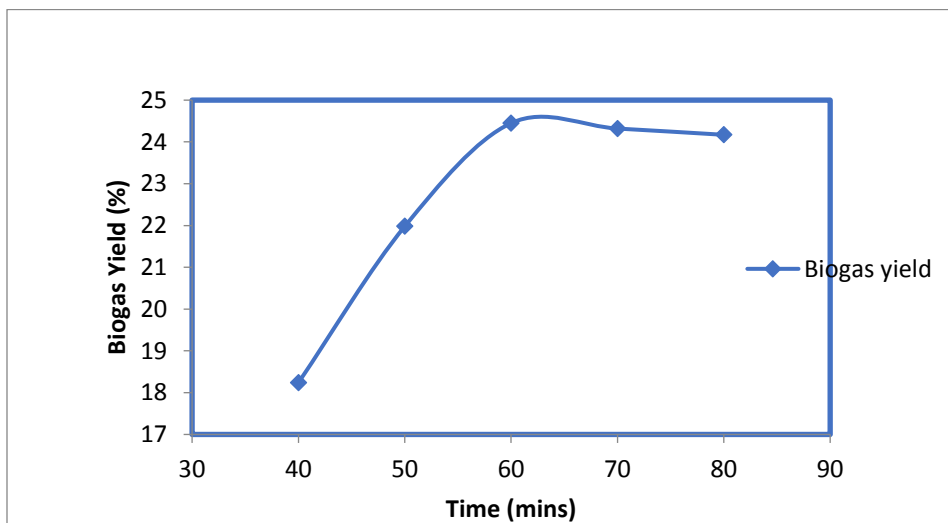
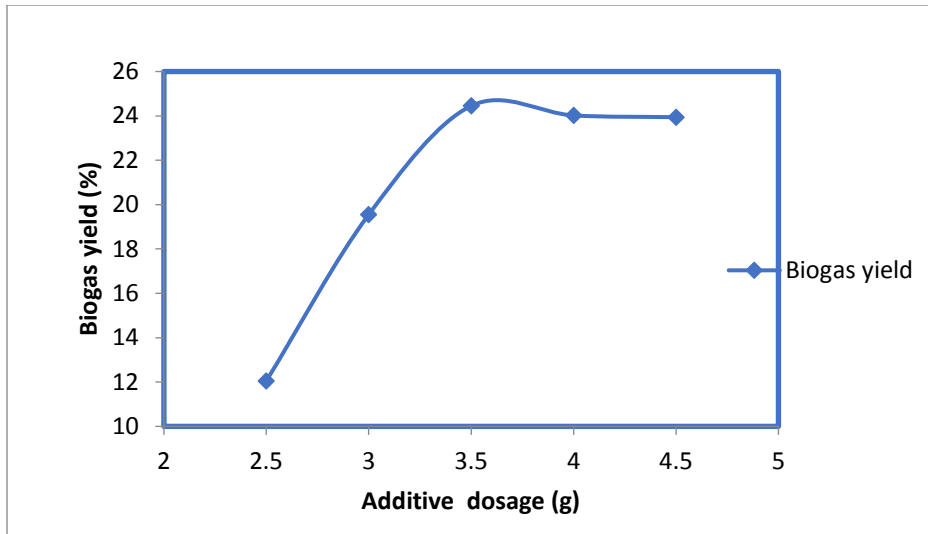
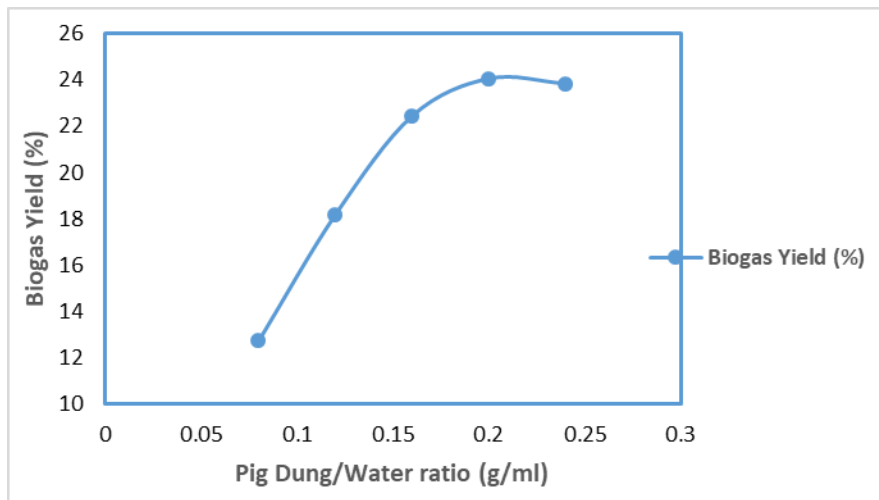


Fig. 5: Effect of time on the biogas yield



**Fig. 6: Effect of Additive dosage on the yield**



**Fig. 7: Effect of pig dung/water ratio on the biogas yield**

### 3.4 Optimization with Response Surface Methodology (RSM)

The Central Composite Design (CCD) of Response Surface Methodology (RSM) was employed to design the experiment (DOE) and model the biogas production process under anaerobic conditions. Table 2 outlines the biogas yields achieved from pig dung, considering variations in pig dung-to-water ratios, additive dosages, temperatures, and digestion times, as specified by the experimental design. The results indicate that the highest cumulative biogas yield of 24.45% was achieved with a substrate-to-water ratio of 0.16 g/mL, an additive dosage of 3.5 g, at a temperature of 70°C for 60 minutes. Conversely, the lowest cumulative yield of 17.56% was recorded at a substrate-to-water ratio of 0.4 g/mL, an additive dosage of 3 g, at 50°C for 60 minutes.

The Model F-value of 124.50 indicates that the model is highly significant. As shown in Table 4, there is only a 0.01% probability that such a large F-value could result from random noise. Model terms with p-values less than 0.0500 are considered significant, while those with p-values greater than 0.05 are deemed insignificant. In this analysis, the significant model terms include A, B, C, D, AB, AD, BD, A<sup>2</sup>, B<sup>2</sup>, C<sup>2</sup>, and D<sup>2</sup>. The Predicted R<sup>2</sup> value of 0.9049 aligns reasonably well with the Adjusted R<sup>2</sup> value of 0.9681, as the difference between them is less than 0.2. Adeq Precision, which measures the signal-to-noise ratio, is 25.507, well above the desirable threshold of 4, indicating a strong signal. This model is suitable for navigating the design space. Additionally, the model used for this process is statistically significant, with a p-value of less than 0.0001.

Table 4 presents the estimated statistical parameters used to assess the model's fitness. The values of  $R^2$ , Adjusted  $R^2$ , and Predicted  $R^2$  are close to 1, indicating that the experimental results are reliable and consistent (Iweka et al., 2021). The coefficient of determination ( $R^2$ ) of 0.9835 suggests that the model accounts for 98.35% of the variability in the response, further supporting the reliability of the findings. The Predicted  $R^2$  of 0.9049 aligns well with the Adjusted  $R^2$  of 0.9681, as their difference is less than 0.2. The model source had a Sum of Squares value of 124.50. Each regression source had a degree of freedom (DF) of one, contributing to a total DF of 14 for the model source. The Mean Squares of the model was calculated as 8.89 by dividing the Sum of Squares by the corresponding DF.

**Table 3 Biogas Yield Under Varying Conditions**

		<b>Factor 1</b>	<b>Factor 2</b>	<b>Factor 3</b>	<b>Factor 4</b>	<b>Response</b>
<b>Std Run</b>		<b>A:pig dung/water ratio</b>	<b>B:Additive dosage</b>	<b>C:Time</b>	<b>D:Temp.</b>	<b>Biogas yield</b>
		<b>(g/ml)</b>	<b>(g)</b>	<b>(mins)</b>	<b>(°C)</b>	<b>(%)</b>
5	1	0.12	3	70	60	20.87
16	2	0.20	4	70	80	24.08
29	3	0.16	3.5	60	70	24.45
12	4	0.20	4	50	80	23.93
18	5	0.24	3.5	60	70	21.20
1	6	0.12	3	50	60	17.56
2	7	0.20	3	50	60	18.77
4	8	0.20	4	50	60	19.38
3	9	0.12	4	50	60	18.65
15	10	0.12	4	70	80	21.51
17	11	0.08	3.5	60	70	18.40
6	12	0.20	3	70	60	21.36
28	13	0.16	3.5	60	70	24.45
8	14	0.20	4	70	60	22.95
19	15	0.16	2.5	60	70	21.20
27	16	0.16	21	60	70	24.45
13	17	0.12	3	70	80	20.94
11	18	0.12	4	50	80	21.63
10	19	0.20	3	50	80	24.09
30	20	0.16	3.5	60	70	24.45
21	21	0.16	3.5	40	70	21.71
20	22	0.16	4.5	60	70	22.47
25	23	0.16	3.5	60	70	24.45
23	24	0.16	3.5	60	50	21.19
24	25	0.16	3.5	60	90	24.35
22	26	0.16	3.5	80	70	23.81
7	27	0.12	4	70	60	22.10
14	28	0.20	3	70	80	23.39
9	29	0.12	3	50	80	21.74
26	30	0.16	3.5	60	70	24.45

**Table 4: ANOVA for Quadratic Model of The Biogas Yield**

Source	Sum of Squares	df	Mean Square	F Value	p-value Prob > F
Model	124.50	14	8.89	63.83	< 0.0001 Significant
<i>A-PD-H2O</i>	14.36	1	14.36	103.09	< 0.0001
<i>B-Add. dos.</i>	2.69	1	2.69	19.30	0.0005
<i>C-time</i>	10.25	1	10.25	73.56	< 0.0001
<i>D-temp.</i>	28.40	1	28.40	203.86	< 0.0001
<i>AB</i>	6.473E-005	1	6.473E-005	4.646E-004	0.9831
<i>AC</i>	2.799E-003	1	2.799E-003	0.020	0.8892
<i>AD</i>	2.57	1	2.57	18.43	0.0006
<i>BC</i>	0.43	1	0.43	3.11	0.0983
<i>BD</i>	0.78	1	0.78	5.57	0.0323
<i>CD</i>	12.92	1	12.92	92.76	< 0.0001
<i>A<sup>2</sup></i>	41.11	1	41.11	295.03	< 0.0001
<i>B<sup>2</sup></i>	14.00	1	14.00	100.50	< 0.0001
<i>C<sup>2</sup></i>	6.41	1	6.41	46.01	< 0.0001
<i>D<sup>2</sup></i>	6.11	1	6.11	43.83	< 0.0001
Residual	2.09	15	0.14		
<i>Lack of Fit</i>	2.09	10	0.21		
<i>Pure Error</i>	0.000	5	0.000		
Cor Total	126.59	29			
Std. Dev.	0.37		R-Squared	0.9835	
Mean	22.13		Adj R-Squared	0.9681	
C.V. %	1.69		Pred R-Squared	0.9049	
PRESS	12.04		Adeq Precision	25.507	

**3.4.1 Final Equation in Terms of Coded Factors:**

A regression equation, expressed in terms of coded factors, was formulated to define the mathematical relationship between the biogas yield from anaerobic digestion and various independent process variables.

$$\text{Biogas yield} = +24.45 + 0.77*A + 0.33*B + 0.65*C + 1.09*D - 2.011E^{-0.003}*AB - 0.013*AC + 0.40*AD + 0.16*BC - 0.22*BD - 0.9*CD - 1.22*A^2 - 0.71*B^2 - 0.48*C^2 - 0.47*D^2 \quad (10)$$

The equation expressed in terms of coded factors allows for predicting the response based on specific levels of each factor. This coded equation is particularly valuable for assessing the relative influence of the factors by analyzing and comparing their coefficients.

In Fig. 8 the data points closely follow the 45-degree diagonal line, suggesting a strong agreement between predicted and actual values. This indicates that the developed RSM model has high accuracy in predicting biogas yield. The points are color-coded, possibly indicating yield magnitude (blue for lower values, red for higher values). The smooth color transition further confirms a well-fitted model. The tight clustering of points suggests a low error margin and high predictive reliability. The high  $R^2$  value (close to 1.0) would quantitatively confirm the goodness of fit.

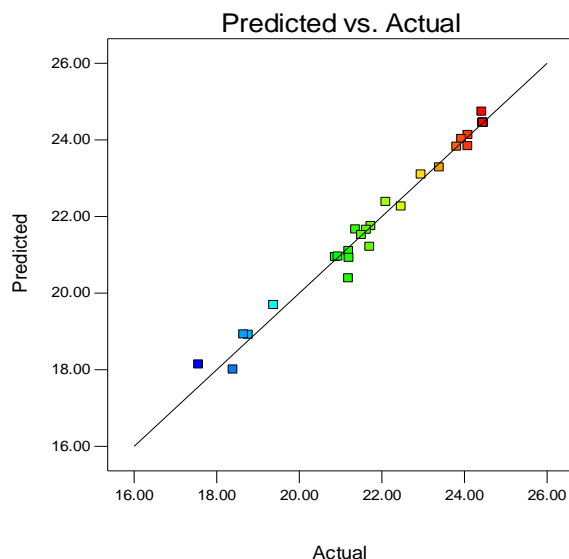


**Fig. 8: Plot of predicted versus actual biogas yield**

Fig. 9 present the influence of time and temperature on the response (% biogas yield). The concavity of the 3D RSM plot indicates that time and temperature need to be optimized simultaneously. With an increase in temperature, the response increases to a maximum and then stabilizes or decreases (yellow to red zones). This is in line with kinetic theory, with increasing reaction rates at temperature until an optimum at which point thermal degradation lowers efficiency. The response increases with increasing time at first, suggesting increased reaction times make the process better (e.g., improved breakdown of substrate to produce biogas). Excessive temperatures and prolonged exposure time result in decreasing response due to potential inhibition effects. The contour projection (bottom view) confirms this trend with an optimal area (yellow/red areas) where temperature and time are balanced for peak output.

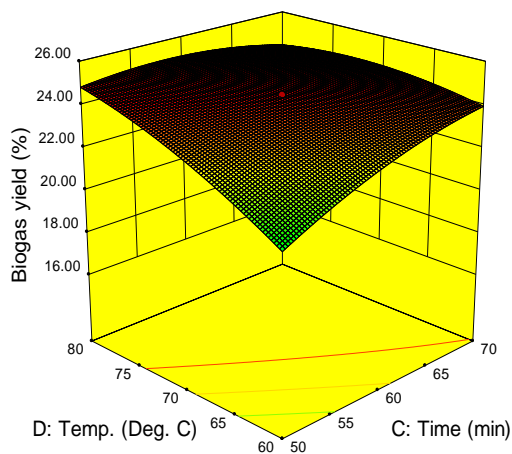


**Fig. 9: Three-dimensional plot of biogas yield versus temperature and time**

### 3.5 Determination of Biogas Quality, Composition and Characterization using FTIR

Table 5 displays the composition of biogas generated from pig dung using snail shell as an additive. The biogas components are listed with their concentration (in  $\mu\text{g/ml}$ ) and corresponding percentage concentration in the total gasmixture. The high percentage of methane indicates efficient anaerobic digestion and a good-quality biogas yield. Methane is the primary combustible gas in biogas and determines its energy value. Carbon Dioxide ( $\text{CO}_2$ )

is the Second Most Abundant Gas (27.26%) and is a natural byproduct of anaerobic digestion. A moderate CO<sub>2</sub> percentage is expected in biogas. Some pre-treatment methods (e.g., scrubbing) can remove CO<sub>2</sub> to improve biogas purity. Acetic Acid and Lactic Acid are intermediate end products of microbial fermentation. Their occurrence is a sign of an ongoing phase of acetogenesis, which ultimately leads to methane production. Phenol is a byproduct of microbial decomposition of organic matter, the low percentage here shows minimal inhibition. Ethylene is usually a trace component in biogas while the occurrence of Ethanol points to the incomplete breakdown of organic material, possibly as a result of sluggish microbial breakdown of alcohols. H<sub>2</sub>S is a common impurity in biogas, produced from sulfur-containing organic matter. Snail shell, being calcium-rich, may have helped to buffer H<sub>2</sub>S levels via neutralization of acid byproducts. Acetonitrile is an uncommon component in biogas and may be derived from nitrogenous feedstock compounds. Its low concentration means minimal impact on biogas quality as a whole.

**Table 5. Biogas from pig dung using snail shell as additive**

Components	Concentration(ug/ml)	% Concentration
Lactic acid	0.0109	0.011
Methane	66.2454	66.908
Acetic Acid	1.1766	1.188
CO <sub>2</sub>	26.9856	27.255
Phenol	0.6422	0.647
Ethylene	1.8135	1.832
Ethanol	0.0014	0.001
Acetonitrile	0.3207	0.324
Hydrogen Sulphide	1.8137	1.832
TOTAL	99.0100	100

In table 6, The strong peaks around 2900 cm<sup>-1</sup> confirm methane as a dominant component, which is good for energy production. The peak around 2350 cm<sup>-1</sup> suggests CO<sub>2</sub> presence, which may lower the biogas calorific value if in excess. The broad peak at 3500 cm<sup>-1</sup> indicates water vapor, which may need to be removed for better combustion efficiency. The peaks around 1200-1300 cm<sup>-1</sup>, suggests H<sub>2</sub>S contamination, which requires desulfurization to prevent corrosion. Peaks in the 1000–1750 cm<sup>-1</sup> range suggest trace organic compounds like acetic acid, phenols, or aldehydes, which result from anaerobic digestion.

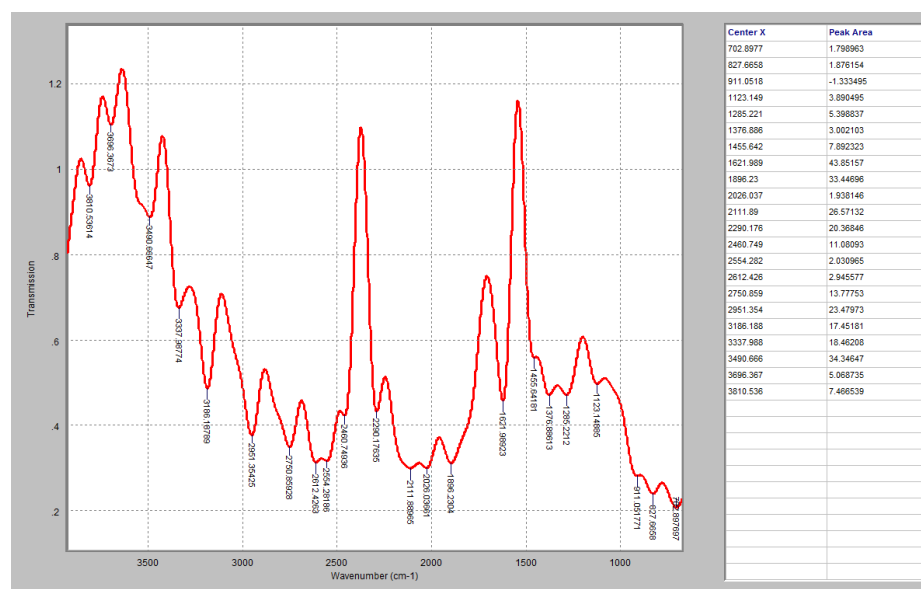


**Fig. 10: FTIR result of biogas yield**

**Table 6. Functional Group and Wavelength of Produced Biogas (Iweka et al., 2021).**

Functional group	Wavelength (Range)	Wavelength (Actual)	Vibrational motion
Alcohol,Hydroxy and water vapour(H <sub>2</sub> O)	3800-3200	3186.188, 3337.988, 3490.666, 3696.367, 3810.536	O-H stretch
Aliphatic alkene/alkyl	3000-2800	2750.859	C-H Stretch
Methylene	2935-2915	2951.354	C-H Stretch
Carboxylic acids	3400-2200	2290.176, 2460.749, 2554.282	O-H stretch
Methylene	2860-2610	2612.426, 2750.859	C-H Stretch
Isothiocyanate	2150-1890	1896.23, 2026.037, 2111.89,	-NCS Stretch
Carboxylic acid	1400-1650	1455.642, 1621.989,	C-O Stretch
Methyl	1380-1370	1376.886	C-H Bend
Aliphatic alkyl	1300-700	702.8977, 827.6658, 911.0518, 1123.149, 1285.221	C-C Vibrations

#### 4.0. Conclusion

The thermophilic production of biogas from anaerobic digestion pig dung with introduction of snail shell as an additive will produce clean and safer energy. The proximate analysis of pig dung (PD) suggests that it is a highly suitable feedstock for biogas production due to its rich organic content, significant energy value, low ash, and fixed carbon. However, moisture levels may require adjustment to optimize microbial activity. The presence of high quantity of carbon carbonate in the snail shell as deduced from the XRD, FTIR AND XRF analysis makes it valuable additive for biogas production leading to higher methane yield. This study shows that the optimal conditions for biogas production were additive dosage at 3.5 g, pig dung/ water ratio at 0.16 g/ml, time at 60 mins and temperature at 70 °C, under these conditions the biogas yield was 24.45 %. The biogas yield is influenced by factors such as the pig dung-to-water ratio, digestion time, temperature, and additive dosage, as demonstrated by the ANOVA results. The model used in this study is statistically significant, with a p-value of less than 0.0001. The R<sup>2</sup> value of 0.9835, along with other statistical parameters, indicates that the anaerobic digestion of pig dung for biogas production can be effectively represented by the model.

The produced biogas contains 66.9% methane and 27.2% CO<sub>2</sub> by volume with other constituents as shown by gas chromatography analysis. FTIR analysis of the biogas shows it contains functional groups associated with biogas. Therefore, the feedstocks used in this study have the potential to support large-scale biogas production in an efficient and sustainable manner. Additionally, the digestate generated during the biogas production process serves as a valuable byproduct that can be utilized as fertilizer to enhance soil quality.

#### References

- AOAC, 1990. In K. Helrich (Ed.), Official Methods of Analysis (15th ed.). Arlington, VA, USA: Association of Official Analytical Chemists, Inc. Duncan, B. O.
- APHA, 2005. Standard Methods of Water and Wastewater. 21st Edn., American Public Health Association, Washington, DC., ISBN: 0875530478, pp: 2-61. Boyde, C.E., 2000. Water
- Çalhan, R., Ulutaş, K., 2023. Boosting biogas production and methane yield by using street dust as an additive on anaerobic digestion of cattle manure. Biomass Conversion and Biorefinery, 13(8), 7385-7396.
- Cheng, Y., Yuan, T., Deng, Y., Lin, C., Zhou, J., Lei, Z., Zhang, Z., 2018. Use of sulfur-oxidizing bacteria enriched from sewage sludge to biologically remove H<sub>2</sub>S from biogas at an industrial-scale biogas plant. Bioresource Technology Reports, 3, 43-50.
- Chilakpu, K. O., 2015. Renewable Energy Sources. Its Benefits, Potentials and Challenges in Nigeria. Journal of Energy Technologies and Policy, 5(9).
- Ezekoye, V. A., Ezekoye, B. A., Offor, P. O., 2011. Effect of retention time on biogas production from poultry droppings and cassava peels. Nigerian Journal of Biotechnology, 22, 53-59.
- Gbenebor, O. P., Akpan, E. I., Adeosun, S. O., 2017. Thermal, structural and acetylation behavior of snail and periwinkle shells chitin. Progress in biomaterials, 6, 97-111.

- Generowicz, N., 2020. Overview of selected natural gas drying methods. *Architecture, Civil Engineering, Environment*, 13(3), 73-83.
- Godfrey, O. U., 2024. Renewable Energy from Agricultural Waste: Biogas Potential for Sustainable Energy Generation in Nigeria's Rural Agricultural Communities. *Journal of Engineering Research and Reports*, 26(12), 341-367.
- Ignatowicz, K., Filipczak, G., Dybek, B., Wałowski, G., 2023. Biogas Production Depending on the Substrate Used: A Review and Evaluation Study—European Examples. *Energies*, 16(2), 798.
- International Energy Agency. 2021. Energy policies of IEA countries: review. Paris
- Itodo, I. N., Awulu, J. O., Philip, T., 2001. A comparative analysis of biogas yield from poultry, cattle and piggery wastes. In *Livestock Environment VI, Proceedings of the 6th International Symposium 2001* (p. 402). American Society of Agricultural and Biological Engineers.
- Iweka, S. C., Owuama, K. C., Chukwunke, J. L., Falowo, O. A., 2021. Optimization of biogas yield from anaerobic co-digestion of corn-chaff and cow dung digestate: RSM and python approach. *Heliyon*, 7(11).
- Kaewdang, S., Nirunsin, R., 2019. Synthesis of calcium oxide from river snail shell as a catalyst in production of biodiesel. *Applied Environmental Research*, 41(1), 31-37.
- Kasinath, A., Fudala-Ksiazek, S., Szopinska, M., Bylinski, H., Artichowicz, W., Remiszewska-Skwarek, A., Luczkiewicz, A., 2021. Biomass in biogas production: Pretreatment and codigestion, *Renewable and Sustainable Energy Reviews*, Volume 150, 111509, ISSN 1364-0321.
- KeChrist, O., Sampson, M., Golden, M., Nwabunwanne, N., 2017. Slurry utilization and impact of mixing ratio in biogas production. *Chemical Engineering & Technology*, 40(10), 1742-1749.
- Khalil, M., Berawi, M. A., Heryanto, R., Rizalie, A., 2019. Waste to energy technology: The potential of sustainable biogas production from animal waste in Indonesia. *Renewable and Sustainable Energy Reviews*, 105, 323-331.
- Kuttner, P., Weißböck, A. D., Leitner, V., Jäger, A., 2015. Examination of commercial additives for biogas production. *Agronomy Research*, 13(2).
- Labatut, R. A., Angenent, L. T., Scott, N. R., 2014. Conventional mesophilic vs. thermophilic anaerobic digestion: a trade-off between performance and stability. *Water research*, 53, 249-258.
- Liu, G. L., Kazarian, S. G., 2022. Recent advances and applications to cultural heritage using ATR-FTIR spectroscopy and ATR-FTIR spectroscopic imaging. *Analyst*, 147(9), 1777-1797.
- Liu, M., Wei, Y., and Leng, X., 2021. Improving biogas production using additives in anaerobic digestion: A review. *Journal of Cleaner Production*, 297, 126666.
- Ngumah, C., Ogbulie, J., Orji, J., Amadi, E., 2013. Potential of organic waste for biogas and biofertilizer production in Nigeria. *Environmental research, engineering and management*, 63(1), 60-66.
- Ning, J., Zhou, M., Pan, X., Li, C., Lv, N., Wang, T., Zhu, G., 2019. Simultaneous biogas and biogas slurry production from co-digestion of pig manure and corn straw: Performance optimization and microbial community shift. *Bioresource Technology*, 282, 37-47.
- Ofomatah, A. C., Ugwu, K. E., Ani, J. U., 2021. Biogas production and storage from pig dung co-digested with pineapple peel. In *IOP Conference Series: Earth and Environmental Science* (Vol. 730, No. 1, p. 012004). IOP Publishing.
- Okonkwo, C. C., Edoziuno, F. O., Adediran, A. A., Ibitogbe, E. M., Mahamood, R., Akinlabi, E. T., 2021. Renewable energy in Nigeria: Potentials and challenges. *Journal of Southwest Jiaotong University*, 56(3).
- Onuora, O., Mmesoma, A., N Stephen, U., 2023. Optimization of Process Conditions for the Production of Biogas from Cow Dung. *Journal of Materials Science Research and Reviews*, 11(4), 1-12.
- Owoyemi, H. T., Owoyemi, A. G., 2020. Chemical and phase characterization of snail shell (*Archachatina Marginata*) as bio-waste from South-West in Nigeria for industrial applications. *Chemistry and Materials Research*, 12(6), 15-20.
- Rao, A. P., Jenkins, P. R., Auxier, J. D., Shattan, M. B., Patnaik, A. K., 2022. Analytical comparisons of handheld LIBS and XRF devices for rapid quantification of gallium in a plutonium surrogate matrix. *Journal of Analytical Atomic Spectrometry*, 37(5), 1090-1098.
- Ryue, J., Lin, L., Kakar, F. L., Elbeshbishy, E., Al-Mamun, A., Dhar, B. R., 2020. A critical review of conventional and emerging methods for improving process stability in thermophilic anaerobic digestion. *Energy for Sustainable development*, 54, 72-84.
- Sambo, A. S., Garba, B., Danshehu, B. G., 1995. Effect of some operating parameters on biogas production rate. *Renewable Energy*, 6(3), 343-344.
- Sundalian, M., Husein, S. G., Putri, N. K. D., 2021. Analysis and benefit of shells content of freshwater and land snails from gastropods class. *Chem*, 12(10), 508-517.

- Udomkan, N., Limsuwan, P., 2008. Temperature effects on freshwater snail shells: *Pomacea canaliculata* Lamarck as investigated by XRD, EDX, SEM and FTIR techniques. *Materials Science and Engineering: C*, 28(2), 316-319.
- Wang, Y. M., Tang, D. D., Zhang, X. H., Uchimiya, M., Yuan, X. Y., Li, M., Chen, Y. Z., 2019. Effects of soil amendments on cadmium transfer along the lettuce-snail food chain: Influence of chemical speciation. *Science of the Total Environment*, 649, 801-807.
- Wellington, A., Baraza, L. D., Mageto, M., Oori, K. F., 2017. Energy evaluation and qualitative analysis of biogas produced from co-digesting kitchen waste and cow dung.
- Wu, D., Li, L., Zhao, X., Peng, Y., Yang, P., Peng, X., 2019. Anaerobic digestion: A review on process monitoring. *Renewable and Sustainable Energy Reviews*, 103, 1-12.
- Zhang, X., Witte, J., Schildhauer, T., Bauer, C., 2020. Life cycle assessment of power-to-gas with biogas as the carbon source. *Sustainable Energy & Fuels*, 4(3), 1427-1436.
- Zhou, S., Yuan, Z., Cheng, Q., Weindorf, D. C., Zhang, Z., Yang, J., Xie, S., 2020. Quantitative analysis of iron and silicon concentrations in iron ore concentrate using portable X-ray fluorescence (XRF). *Applied Spectroscopy*, 74(1), 55-62.
- Zuliantoni, Z., Suprpto, W., Setyarini, P. H., Gapsari, F., 2022. Extraction and characterization of snail shell waste hydroxyapatite. *Results in Engineering*, 14, 100390.